LASER INTERFEROMETER GRAVITATIONAL WAVE OBSERVATORY
- LIGO -
CALIFORNIA INSTITUTE OF TECHNOLOGY
MASSACHUSETTS INSTITUTE OF TECHNOLOGY

Technical Note	**LIGO-T1600159-v1**	2016/10/31

LIGO SURF 2016 - Final Paper : Noise Hunting in Advanced LIGO

Michael Antia, Jessica McIver, T.J. Massinger, Alan Weinstein

Distribution of this document:

LIGO Scientific Collaboration

California Institute of Technology
LIGO Project, MS 18-34
Pasadena, CA 91125
Phone (626) 395-2129
Fax (626) 304-9834
E-mail: info@ligo.caltech.edu

Massachusetts Institute of Technology
LIGO Project, Room NW17-161
Cambridge, MA 02139
Phone (617) 253-4824
Fax (617) 253-7014
E-mail: info@ligo.mit.edu

LIGO Hanford Observatory
Route 10, Mile Marker 2
Richland, WA 99352
Phone (509) 372-8106
Fax (509) 372-8137
E-mail: info@ligo.caltech.edu

LIGO Livingston Observatory
19100 LIGO Lane
Livingston, LA 70754
Phone (225) 686-3100
Fax (225) 686-7189
E-mail: info@ligo.caltech.edu

http://www.ligo.caltech.edu/

Abstract

The Laser Interferometer Gravitational-wave Observatory (LIGO) is designed to detect gravitational waves from energetic astrophysical sources in the universe. During its first observing run, LIGO detected two gravitational wave signals from binary black hole mergers, opening up a new path to astronomy. In order to improve LIGO's detection rate, continuous efforts are made to characterize sources of noise and thereby improve LIGO's sensitivity. This project investigated ground motion as a source of non-linear noise at the LIGO observatories. We observed that high winds with an excess velocity of 20 mph have an impact on the Alignment Sensing and Control (ASC) control loops. We found an increase in ASC noise amplitude at three distinct frequency bands. Time frequency analysis indicated the presence of glitches, or transient noise, with a central frequency of 5 Hz during periods of high wind. The effects of seismic motion on the Length Sensing and Control (LSC) control loops were also studied. We observed that elevated seismic motion in 0.03 to 0.1 Hz band increases the noise levels for LSC and ASC loops controlling for the Power Recycling Cavity (PRC) and the Signal Recycling Cavity (SRC). These results will enable commissioners to isolate and eliminate this effect, improve data quality, and enhance the interferometers' performance and stability.

1 Introduction

On September 14, 2015, for the first time in history, the Advanced LIGO detectors observed a gravitational wave signal from a binary black hole merger (GW150914) [1]. A second gravitational wave signal (GW151226) was detected on December 26, 2015, paving the way for a new era of gravitational-wave astronomy [2]. Gravitational waves were first predicted in 1916 by Albert Einstein, stemming from his general theory of relativity, which was published in 1915. Gravitational waves are "transverse waves of spatial strain that travel at the speed of light, generated by time variations of the mass quadrupole moment of the source" [3]. Due to the small amplitudes of gravitational waves, detecting them requires instrumentation of unprecedented sensitivity. LIGO, a pair of modified Michelson Interferometers with Fabry-Perot resonant cavities, achieved the required sensitivity to make the detection of gravitational waves possible [4]. One of the major challenges in enhancing LIGO's sensitivity consists in identifying, and eliminating or isolating sources of noise - both environmental and instrumental.

Commissioning efforts in characterizing noise and improving strain sensitivity allow LIGO to further enhance its detection range [4]. This enhancement will enable LIGO to detect gravitational waves at a higher rate, from smaller mass sources, and deeper into the Universe. The effect of ground motion on the Alignment Sensing and Control (ASC) control loops and Length Sensing and Control (LSC) control loops for both the Power Recycling Cavity Length (PRCL) and Signal Recycling Cavity Length (SRCL) have an impact on the behavior of the interferometer. The control loops are part of a feedback control loop system which is designed to maintain the position and orientation (pitch and yaw degrees of freedom) of the optics. Maintaining the position and orientation of the optics allows the laser to be in resonance within the interferometer's cavities. It was suspected that non-linear noise induced by excess ground motion was a limiting source of noise during LIGO's first observing run [5].

In this project, eight lock stretches that contained periods of both high and low wind at LIGO Hanford were studied in order to observed the impact high winds has on the ASC control loops. Similarly, eighteen lock stretches that contained varied levels of local ground motion at LIGO Livingston were studied in order to observe the impact of elevated ground motion on the ASC and LSC control loops.

1.1 The ASC and LSC control loops

The Alignment Sensing and Control (ASC) control loops are responsible for sensing and controlling the alignment degrees of freedom of the interferometers. Figure 1 shows a basic schematic of the interferometer and its cavities. CARM, the common arm mode, is defined as the average length of the two interferometer arms:

$$\frac{L_x + L_y}{2} \tag{1}$$

and DARM, the differential arm mode, is defined as the difference of the two interferometer arm lengths:

$$\frac{L_x - L_y}{2} \tag{2}$$

as seen in Figure 1 [6].

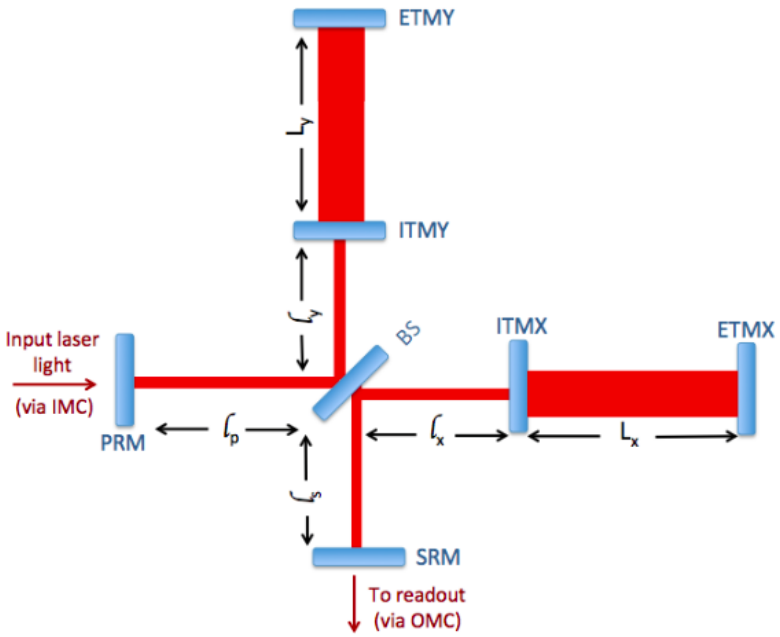

Figure 1: Basic schematic of the interferometer and its cavities. The Beam Splitter (BS), Signal Recycling Mirror (SRM), Power Recycling Mirror (PRM), Input Test Mass X (ITMX) and Input Test Mass Y (ITMY) are all located at the intersection of both 4km arms, or the corner station. The End Test Mass Y (ETMY) and the End Test Mass X (ETMX) are located at the end of the 4km arms, or the end station. Image obtained from Jessica McIver's Dissertation "*The impact of terrestrial noise on the detectability and reconstruction of gravitational wave signals from core-collapsed supernovae.*" UMass Amherst. Scholar Works. Paper 539. (2015)

In addition, the soft and hard modes shown in Figure 2, correspond to the relative angular orientation of the optics.

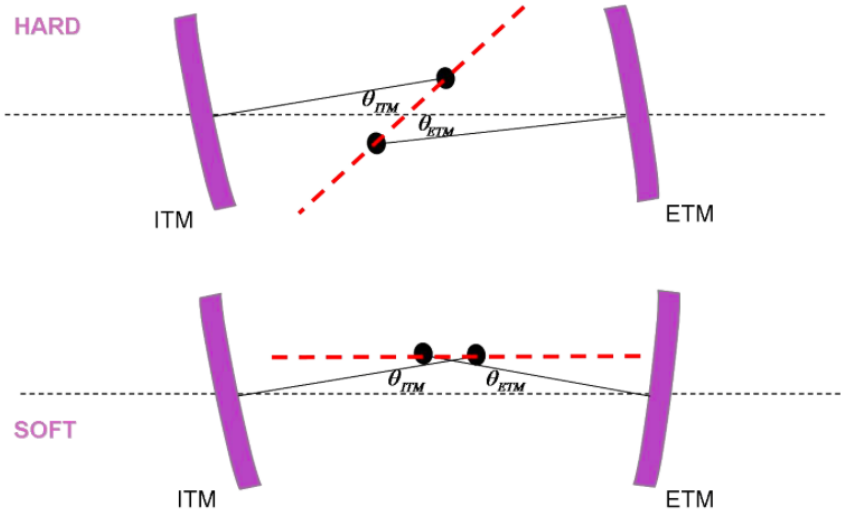

Figure 2: Depiction of hard and soft modes for CARM and DARM. Image obtained from LIGO Document Control Center - DCC # T0900511-v4. L. Barsotti, M. Evans. *Modelling of Alignment Sensing and Control for Advanced LIGO.*

Sixteen channels representing the sensor and control signals for the ASC loops were used in this investigation: :

- H1:ASC-DHARD_P_OUT_DQ
- H1:ASC-DHARD_Y_OUT_DQ
- H1:ASC-DSOFT_P_OUT_DQ
- H1:ASC-DSOFT_Y_OUT_DQ
- H1:ASC-CHARD_P_OUT_DQ
- H1:ASC-CHARD_Y_OUT_DQ
- H1:ASC-CSOFT_P_OUT_DQ
- H1:ASC-CSOFT_Y_OUT_DQ
- H1:ASC-X_TR_A_PIT_OUT_DQ
- H1:ASC-X_TR_A_YAW_OUT_DQ
- H1:ASC-X_TR_B_PIT_OUT_DQ
- H1:ASC-X_TR_B_YAW_OUT_DQ
- H1:ASC-Y_TR_A_PIT_OUT_DQ
- H1:ASC-Y_TR_A_YAW_OUT_DQ
- H1:ASC-Y_TR_B_PIT_OUT_DQ
- H1:ASC-Y_TR_B_YAW_OUT_DQ

The channels on the left column record the pitch and yaw actuation control signal for both soft and hard modes for the CARM and DARM degrees of freedom. The channels on the right column record the transmitter power on the photodiodes for both pitch and yaw angular motion at the X and Y end stations.

In a supplementary study, we observed the effect of elevated ground motion on the pitch and yaw degrees of freedom for the control signal for one of the optics in the signal recycling cavity at LIGO Livingston. We also analyzed the effects on the Length Sensing Control (LSC) loops for the Power Recycling Cavity Length (PRCL) and the Signal Recycling Cavity Length (SRCL) during periods of elevated ground motion.

As shown in Figure 1 on page 2, PRCL is defined as the sum of the distance between the beam splitter and the power recycling mirror and the average of the lengths between the beam splitter and each input test mass:

$$l_p + \frac{(l_x + l_y)}{2} \tag{3}$$

and SRCL as the distance between the beam splitter and the signal recycling mirror and the average of the lengths between the beam splitter and each input test mass optic:

$$ls + \frac{(l_x - l_y)}{2} \tag{4}$$

2 The effect of high winds on the Alignment Sensing and Control loops

2.1 Defining study times

We identified lock stretches that coincided with periods of both high and low wind. We defined high wind periods to be times when local wind speed exceeded 20 mph and low wind periods when wind speed was less than 5 mph. The following times listed below correspond to lock stretches which contained periods of both high and low wind:

Table 1: Lock stretches coincident with periods of both high and low wind.

Date	High Wind Time Segment (UTC)	Low Wind Time Segment (UTC)
September 27, 2015	00:30 - 06:00	15:00 - 16:30
October 09, 2015	17:00 - 21:30	07:30 - 11:00
October 11 - 12, 2015	18:00 - 22:00 (10/11/15)	02:00 - 5:00 (10/12/15)
November 05, 2015	17:30 - 19:30	16:00 - 17:00
November 12, 2015	17:00 - 18:15	15:00 - 16:30
December 14, 2015	17:30 - 19:30	05:00 - 07:00
December 18, 2015	17:00 - 20:00	10:00 - 15:00
December 20, 2015	18:30 - 19:00	00:00 - 12:30

2.2 Amplitude Spectral Density plots

To determine the frequency content of the signal, we generated amplitude spectral density plots of the 16 ASC channels using GWpy, a Python package for data analysis developed for LIGO. During periods of high wind, noise levels increased in three distinct frequency bands: 0-1 Hz, 4-20 Hz, and 20-40 Hz, as seen in Figures 3, 4, 5, & 6. The channels plotted are the most representative of noise increases due to elevated wind speeds of the eight dates analyzed.

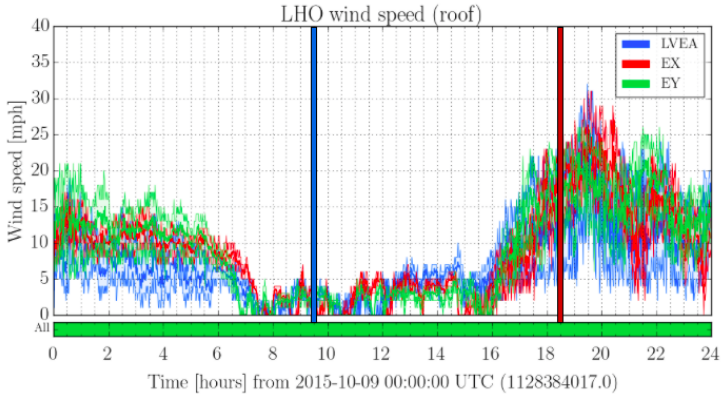

Figure 3: Time series for wind speed at Hanford on October 9, 2015. Blue and red line markers used as reference point of times of low and high wind as seen in the ASD plots.

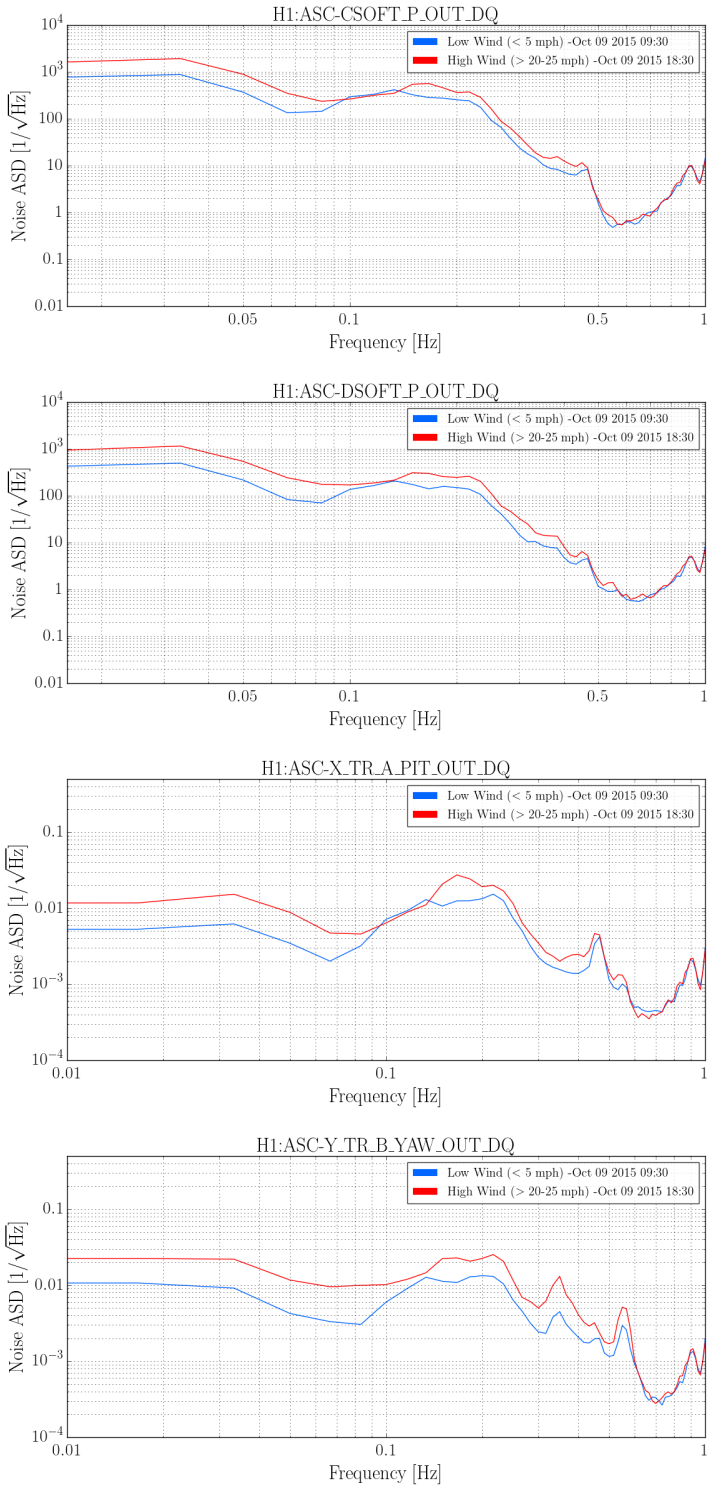

Figure 4: ASD plots of four ASC channels for 0-1 Hz band. At 0.08 Hz, the red trace which represents noise levels during elevated wind speeds, increases almost by a factor of three when compared to the blue trace which serves as a reference for noise levels during low wind. *The Amplitude Spectral Density plots were obtained using GWpy, a Python package for data analysis developed for LIGO[7].*

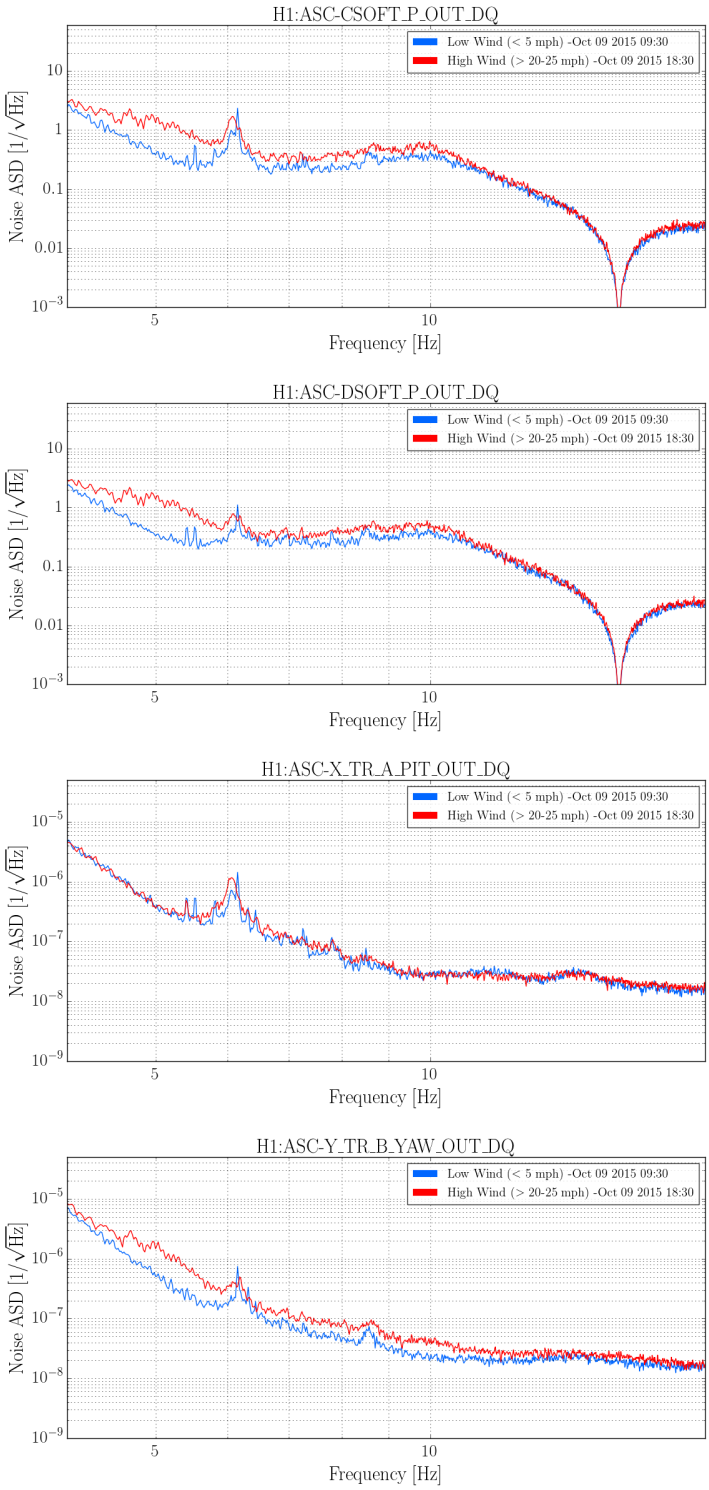

Figure 5: ASD plots of the same four ASD channels for 4-20 Hz band. Glitches with a central frequency of 5 Hz occur in this frequency band. The blue trace serves as a reference for noise levels during low winds and the red trace corresponds to noise levels during elevated wind speeds.

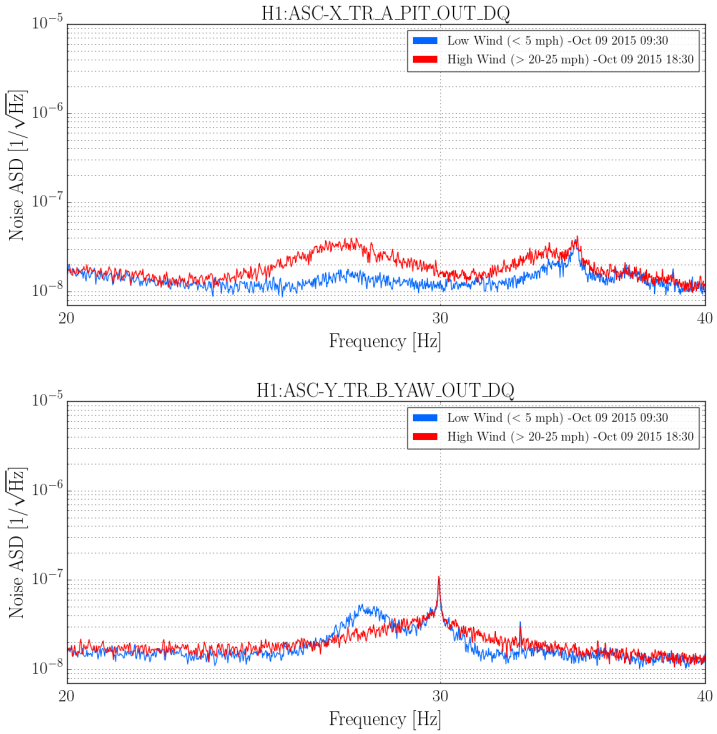

Figure 6: ASD plots of two ASC channels for the 20-40 Hz band. At this frequency band, changes in noise levels were observed only for the transmitted power at the X and Y end stations.

Time lapses were made using ASDs averaged over fifteen minute intervals, which better depict changes in noise levels as wind speed levels change*. An interesting feature observed in the 4-20 Hz band during high wind speeds, as shown in Figure 5, was the presence of a glitch with a central frequency of approximately 5 Hz.

* For an example of a time lapse, please visit: *https://dcc.ligo.org/DocDB/0126/T1600159/001/4_20_Hz_ASD.gif*

2.3 Wind-induced glitches in the ASC loops

A glitch is transient noise well localized in time and frequency. Glitches can be detrimental to searches for astrophysical signals in LIGO data because they can mimic gravitational wave signals. If glitches are abundant and couple into the gravitational wave channel, this results in poor data quality and results in a decrease in gravitational wave search sensitivity.

Although they were not observed to couple to h(t), weaker glitches have the capacity to "raise the background of a search and limit the ability to distinguish signal from noise"[8]. The glitches we observed in the 4-20 Hz band have a central frequency of 5 Hz as seen in Figure 7, which shows spectrograms of several alignment channels when these glitches are present.

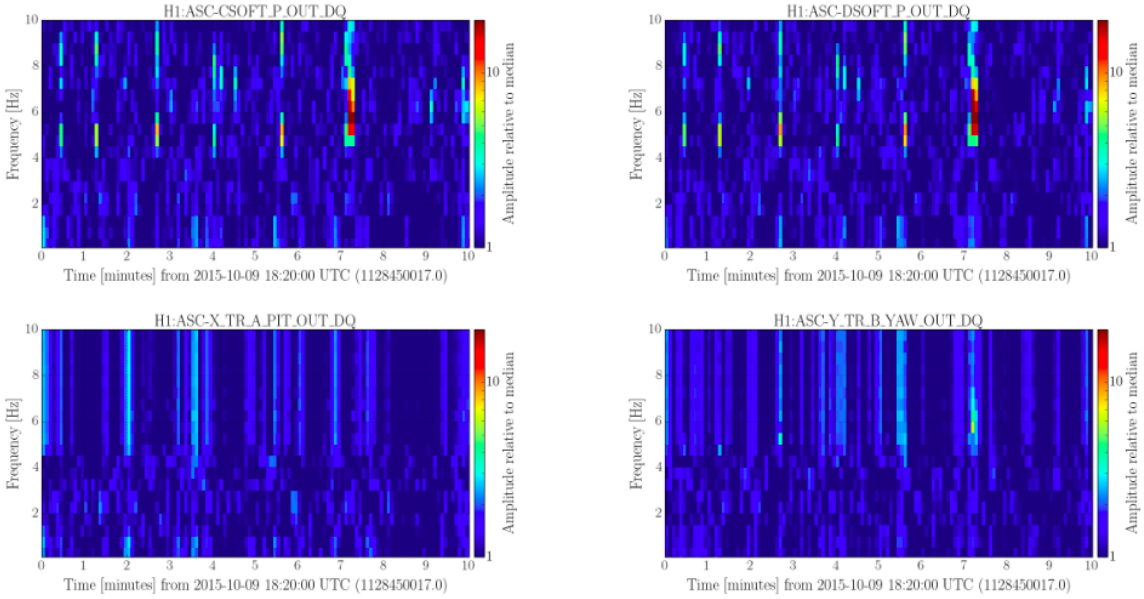

Figure 7: Normalized spectrograms (GWpy) for high wind time segment that demonstrates glitching. Most of the excess power of the glitch occurs around 5 Hz as is indicated by the red segments which have a high amplitude relative to the median.

The glitching observed in Figure 7 is consistent with scattered light. This was better resolved by using an OmegaScan (see Figure 8 below), which shows an arching shape in the time frequency plane, which is indicative of scattered light [9,10].

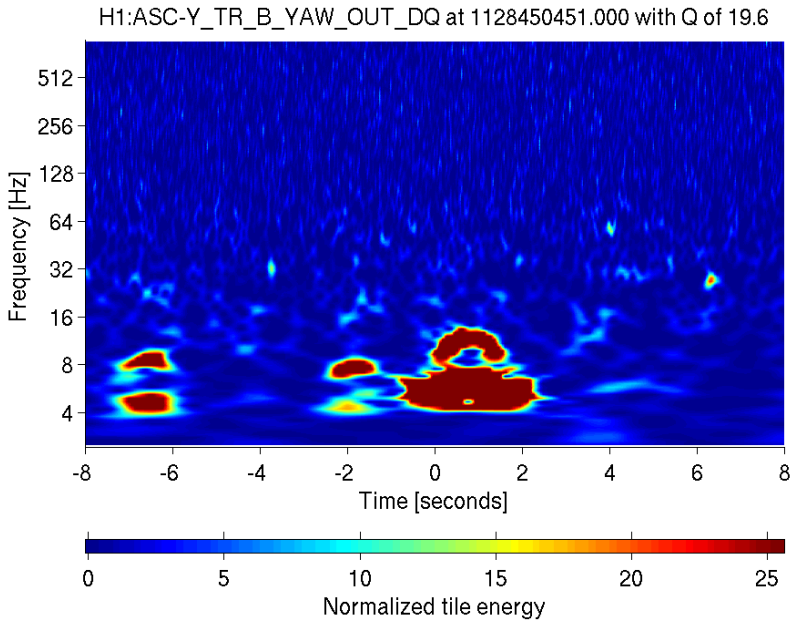

Figure 8: Omega scan showing a glitch with a timestamp centered around 18:27:14 UTC . Arching morphology is indicative of scattered light.

2.4 Do glitches also appear during periods of low wind?

To ensure that the correlation between high winds and 5 Hz glitches was not a false positive, periods of low wind were also examined. Spectrograms for the sixteen ASC control loop channels were plotted for twelve lock stretches during periods of low wind and were compared with band-limited root mean square (BLRMS) velocity trends for ground motion. It was noted that for some of the lock stretches, glitching only appeared during periods of elevated ground motion, as seen in Figure 9. For periods of low wind and relatively low ground motion, we do not see glitches with a central frequency of 5 Hz (see Figure 10).

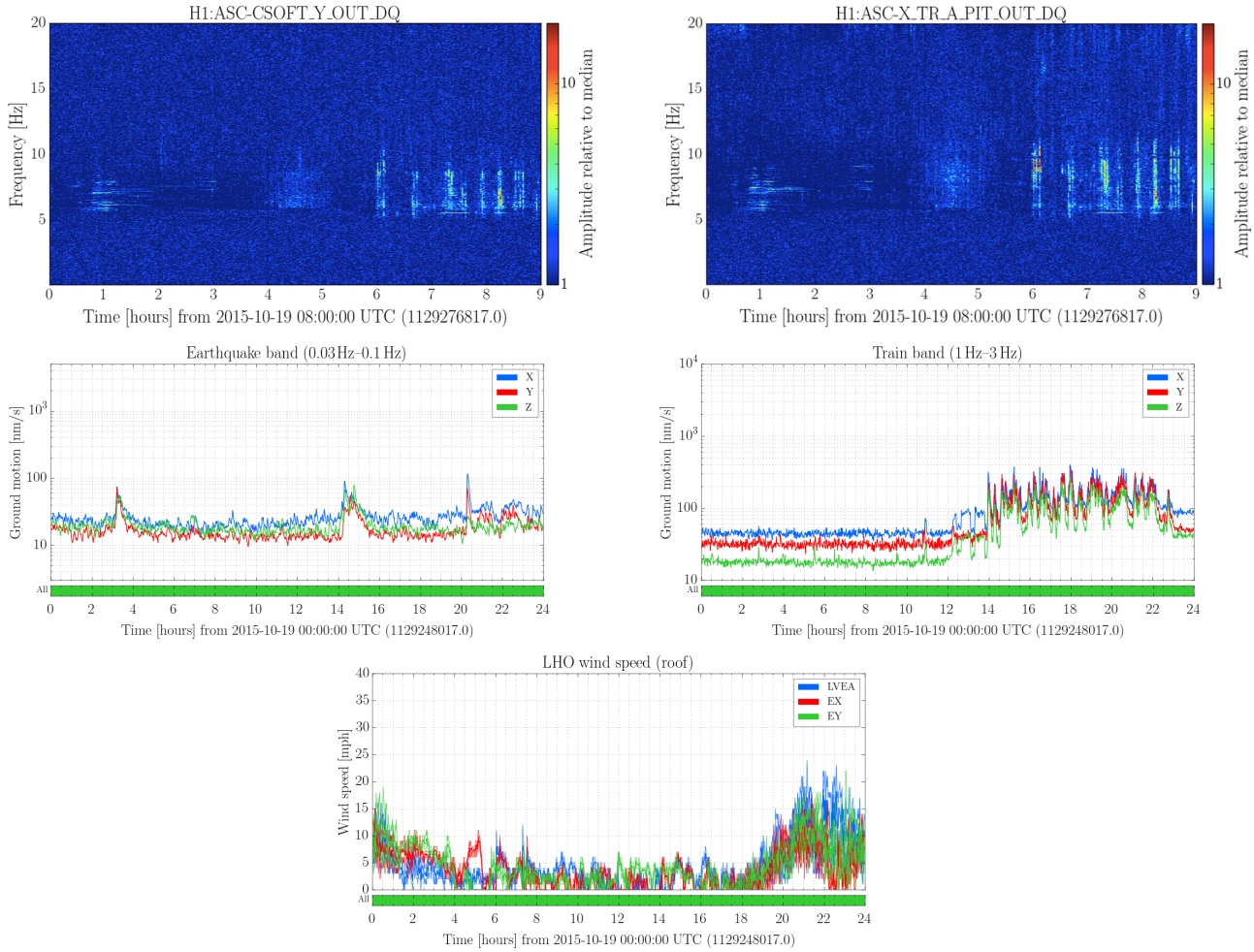

Figure 9: Top row: Normalized spectrograms of representative alignment channels from 8:00 to 17:00 UTC showing excess noise starting at around 14:00 UTC. Middle row: The left plot shows band limited RMS values as a function of time for ground motion in the 0.03-0.1Hz frequency band. The peak that occurs around 14:00 UTC in the earthquake band, correlates with the glitches seen in the spectrograms at 14:00 UTC. The right plot shows band limited RMS values for ground motion in the 1-3 Hz frequency band where we see elevated noise from 14:00 to 23:00 UTC which also may correlate with the glitches in the spectrograms for the time period of 14:00 to 17:00 UTC. Bottom plot: wind speed for same time segment. Wind speeds are relatively low from 08:00 to 19:00 UTC.

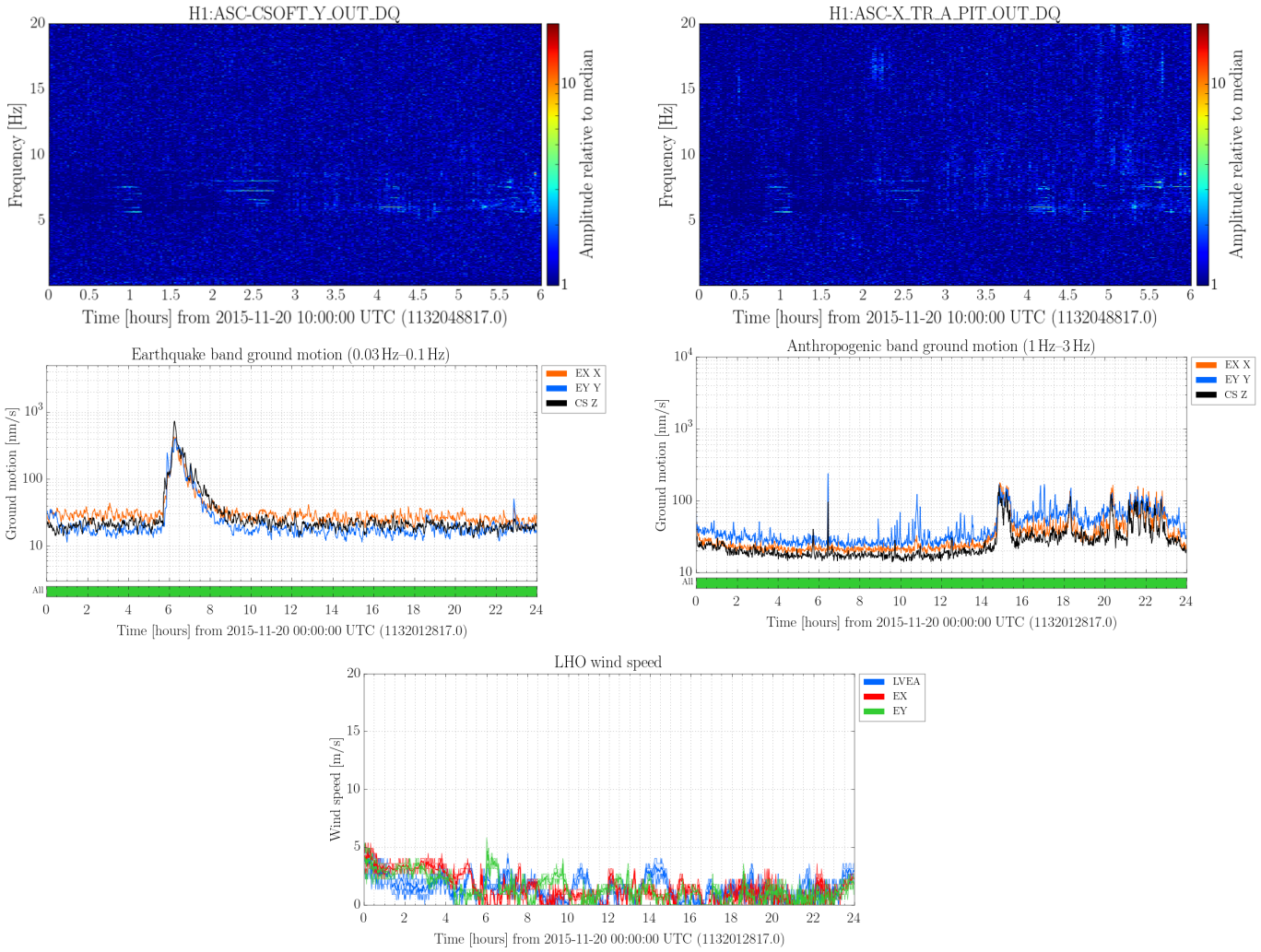

Figure 10: Top row: Normalized spectrograms showing no excess noise in the same alignment channels between 10:00 to 16:00 UTC. Middle row: Band limited RMS values show relatively low ground motion from 10:00 to 16:00 UTC in both 0.03-0.1 Hz and 1-3 Hz frequency bands which is consistent with the lack of glitches in the spectrograms. Bottom plot: wind speed for same time period. Wind speeds are below 5 mph from 10:00 to 16:00.

2.5 Coupling mechanism: ground motion or acoustic vibrations?

The question that remains to be answered is how are the glitches caused by elevated wind propagating to the control loops. One mechanism which was studied was if elevated winds could cause local ground motion directly or indirectly by causing the building to move. The ground motion BLRMS were analyzed for the lock stretches identified in Table 1. Although elevated levels of ground motion coincided with the period of high wind, as seen in Figure 11 on the following page, the amplitude of ground motion induced by high winds were considered too low to warrant ground motion as a coupling mechanism.

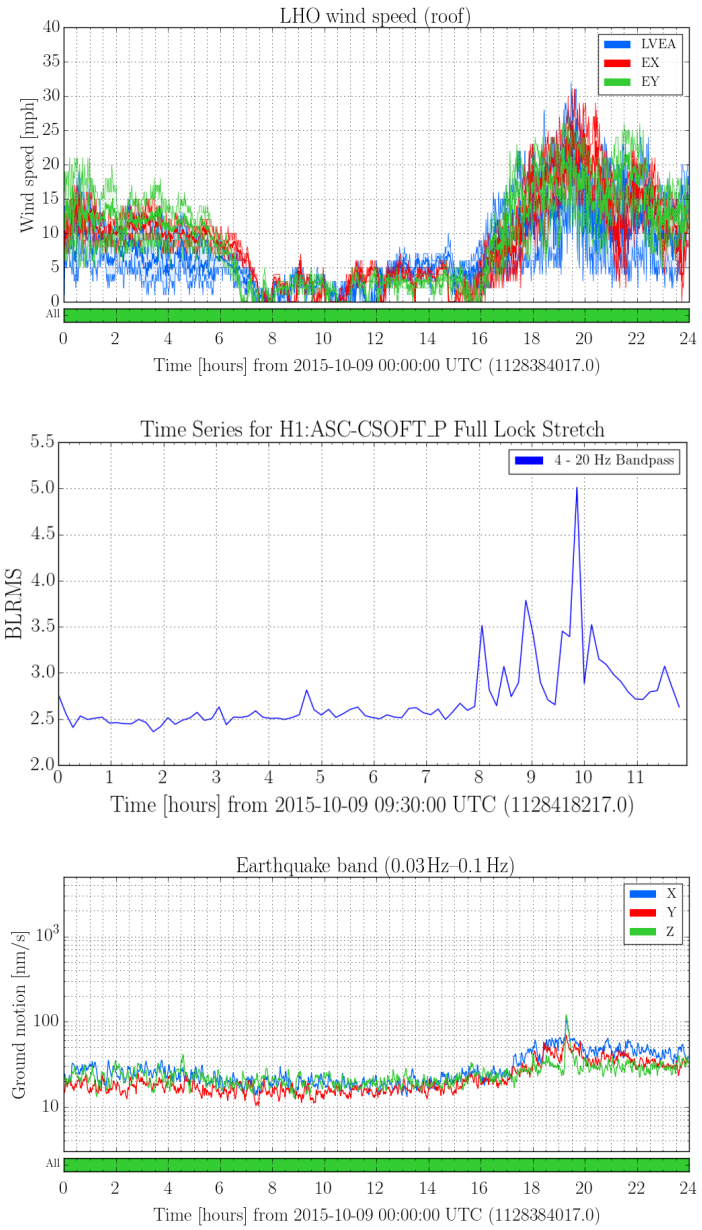

Figure 11: Top plot: Time series for wind speed at Hanford on October 9, 2016. Middle plot: BLRMS for CSOFT pitch degree of freedom. The data for this plot was filtered with a bandpass of 4 to 20 Hz. Notice how well the noise levels for this ASC channel correlate with the elevated wind speed by comparing this plot to the plot above. Bottom plot: Ground motion BLRMS for the earthquake band. The increase of ground motion in the earthquake band during the time of high winds, increases only by a factor of 2.5 or 3.0 which is relatively small and are unlikely to be the coupling mechanism for glitching.

Another possible coupling mechanism is through acoustic vibrations which can couple mechanically to sensitive interferometer components. The Physical Environment Monitor (PEM) microphones which detect acoustic noise were analyzed, and a correlation was observed between high winds and elevated noise levels on the microphones. Though this correlation is apparent as seen in Figure 12 on the following page, acoustic vibrations only correlate with broadband noise and not with glitching in the ASC control loops.

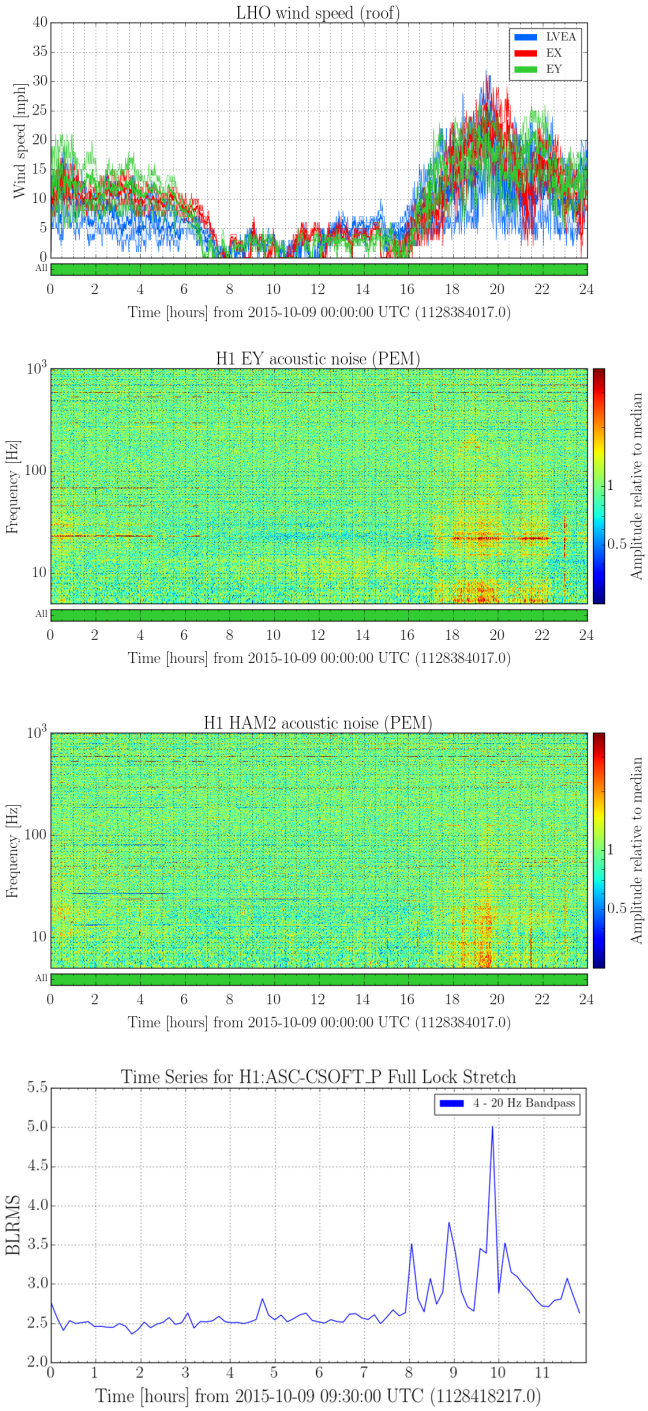

Figure 12: Top plot: Time series for wind speed at Hanford on October 9, 2016. Second plot: Spectrogram for acoustic monitors at the Y end station. Third plot: Spectrogram for acoustic monitors at HAM2, a vacuum chamber located in the corner station. Bottom plot: band-limited RMS of the CSOFT pitch degree of freedom. Note the increase in noise levels in the acoustic spectrograms for frequencies ranging approximately from 2-8 Hz and from 16 Hz all the way to 200 Hz with significant excess power slightly above 20 Hz. at the microphone at the Y end station; and 0-25 Hz at the microphone located at HAM2. Also note the times for which the elevated noise occurs correlates with the time for which high winds were prevalent.

2.6 Concluding remarks

We have observed that an increase in wind speed causes overall elevated noise levels in the ASC channels including glitches with a central frequency of approximately 5 Hz. Though the exact mechanism by which wind is coupling to the interferometer is unknown, acoustic noise tends to correlate well with broadband noise and seems to be a coupling mechanism when comparing the h(t) spectrograms and the microphone spectrograms. Furthermore, we note that elevated wind speeds cause elevated noise in h(t) and a slight drop in the binary neutron star inspiral range as seen in Figure 13.

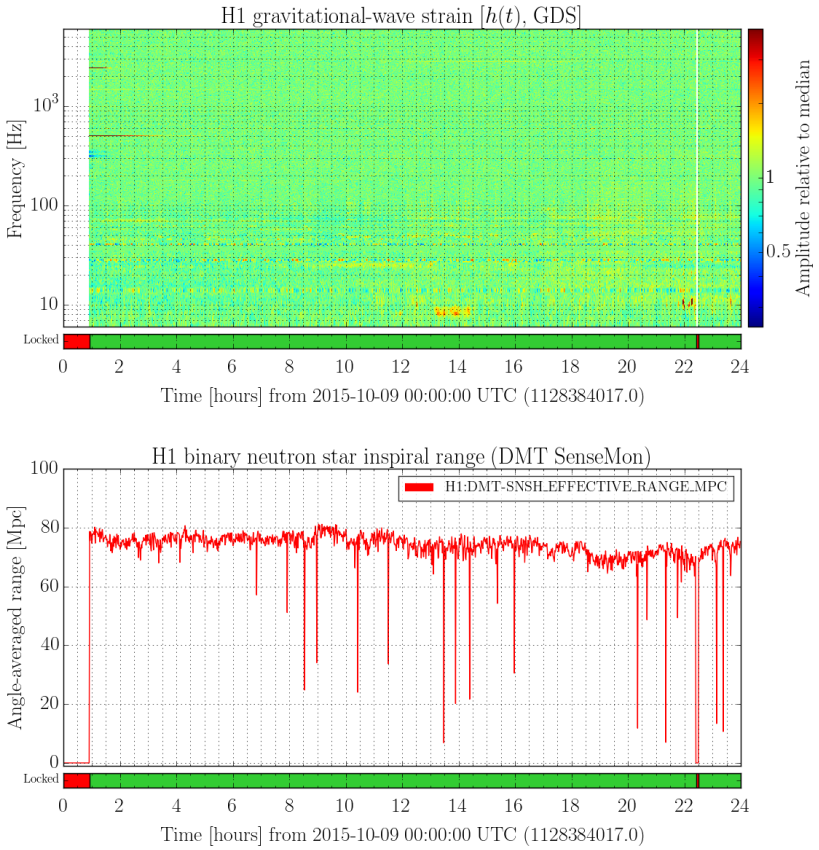

Figure 13: Spectrogram for h(t) and BNS inpiral range for October 9th 2015. Notice the slight drop in the BNS inspiral range at 18:00 UTC which coincides with the period of high wind speed in Figure 12. An increase in noise in h(t) is also evident by the increase of yellow pixelation which corresponds excess power relative to the median. This occurs on the spectrogram at around 17:00 to 22:00 UTC for frequencies ranging from 10 Hz to about 100 Hz.

3 The effect of seismic motion on the Signal Recycling Cavity Length and Power Recycling Cavity Length at the Livingston Observatory

3.1 ASD for PRCL and SRCL

The effect of elevated ground motion on the pitch and yaw degrees of freedom for the control signal for one of the optics in the signal recycling cavity (SRC2) at LIGO Livingston was examined. Using the same time period of elevated ground motion, we analyzed the effects on the Length Sensing Control (LSC) loops for the Power Recycling Cavity Length (PRCL) and the Signal Recycling Cavity Length (SRCL).

Eighteen lock stretches with elevated ground motion at the LIGO Livingston site were identified for the month of November 2015. These dates are:

- 11/02/2015
- 11/03/2015
- 11/04/2015
- 11/05/2015
- 11/06/2016
- 11/09/2015
- 11/11/2015
- 11/12/2015
- 11/13/2015
- 11/15/2015
- 11/16/2015
- 11/20/2015
- 11/21/2015
- 11/23/2015
- 11/24/2015
- 11/28/2015
- 11/29/2015
- 11/30/2015

The overall criteria used in selecting these dates was any distinguishable increases in RMS ground motion for any frequency band: earthquake band, micro-seismic band, anthropogenic band, 3-10 Hz band and 10-30 Hz. Such distinguishable increases could be any increase of a factor of ten to one thousand, for short periods of time (less than 30 minutes) to long periods of time (5 or more hours). ASDs were measured for PRCL and SRCL for all eighteen lock stretches and any outstanding features were noted. In this study, we will focus on the features observed for the day of November 6th, 2015 due to the fact that an interesting glitch feature was observed in the ASD.

Figure 14 shows BLRMS for ground motion for several frequency bands on November 6th. The lock stretch for this day spanned from 00:00 to 16:45 UTC. Our focus was on the time period from 00:00 to 01:45 UTC which corresponds to the time containing elevated ground motion on the earthquake band on the top left plot.

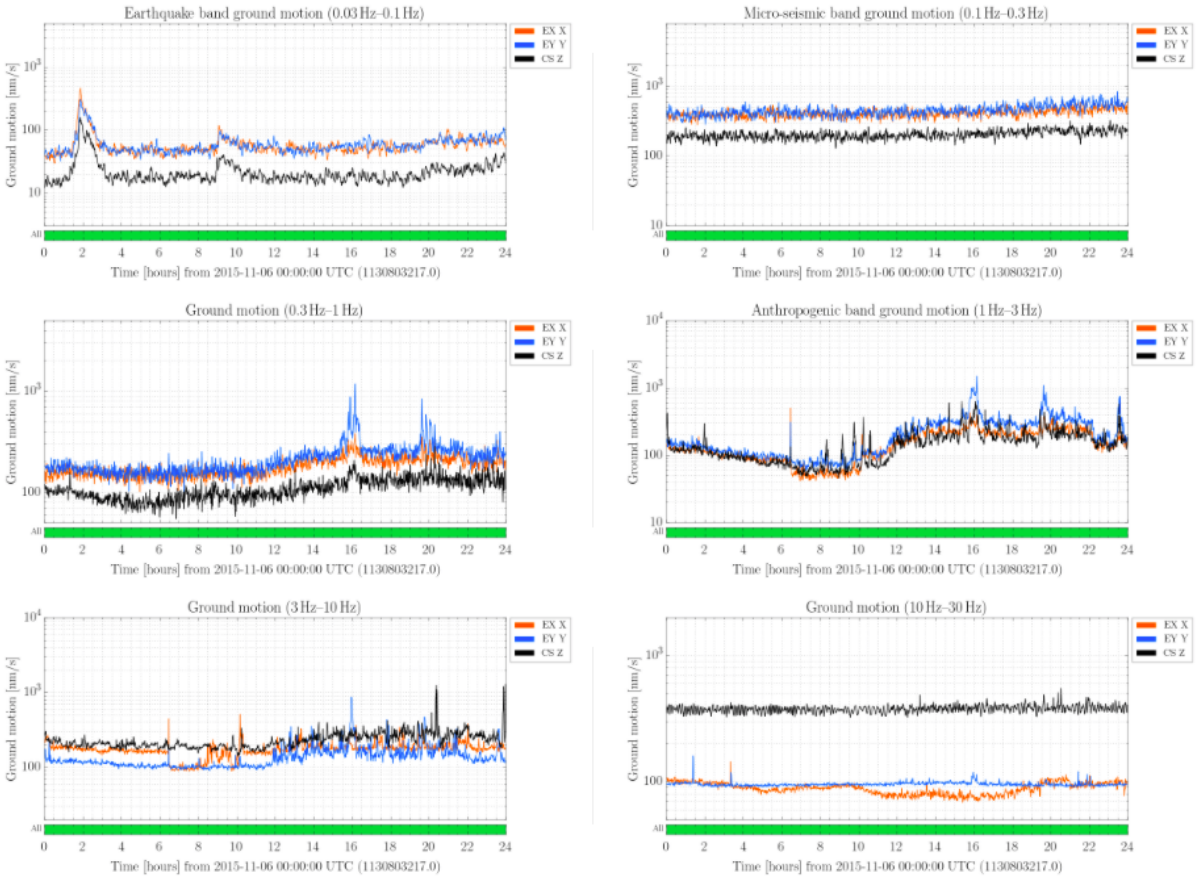

Figure 14: BLRMS for ground motion for different frequency bands at LIGO-Livingston on November 6, 2015.

The fifteen minute averaged ASD for PRCL and SRCL are shown in Figure 15. Elevated ground motion caused an increase in noise levels for frequencies 0.02-0.3 Hz and around 10 Hz. An omega scan centering on this time period resolved glitches at 10 Hz, as will be seen in the following section.

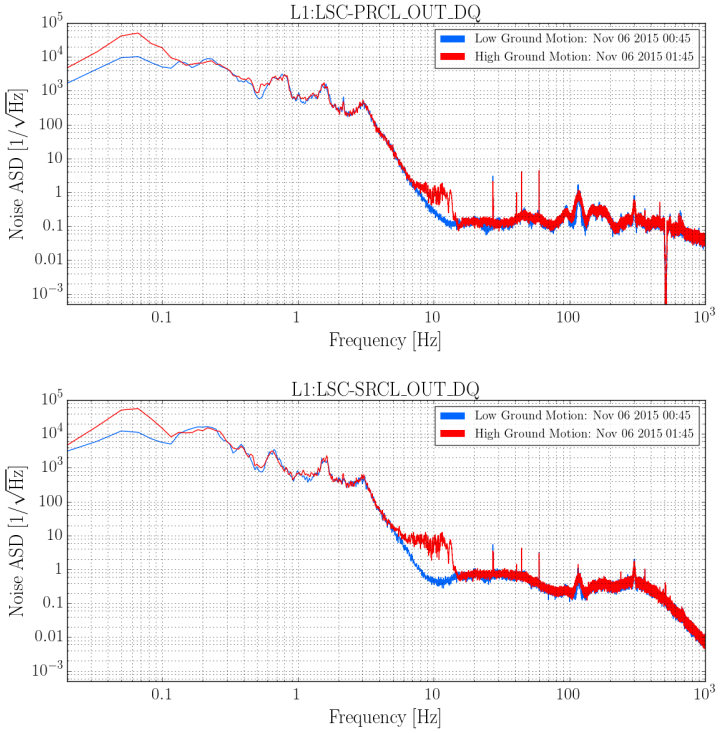

Figure 15: ASD for PRCL and SRCL. The blue trace is a reference for a period of low ground motion, and the red trace is representative of increase in noise levels during elevated ground motion. Notice the excess noise from 7 to 15 Hz, which is indicative of glitching.

3.2 Glitches in PRCL and SRCL

Figure 16 shows normalized spectrograms for PRCL and SRCL.

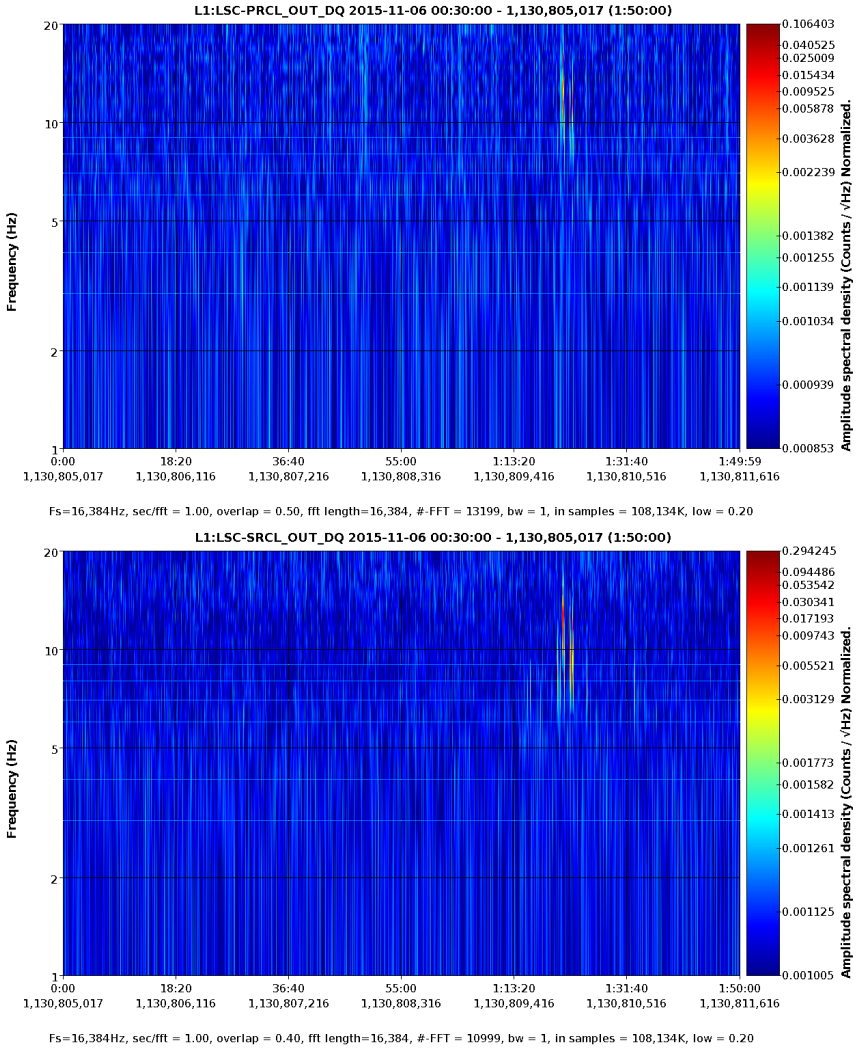

Figure 16: Normalized spectrogram for PRCL (left) and SRCL (right).

Glitches with a central frequency of around 10 Hz are visible in both PRCL and SRCL which coincides with the time of elevated ground motion seen in the earthquake band in Figure 14. Figure 17 shows OmegaScans centered on glitches in both PRCL and SRCL.. The morphology of these glitches is representative of scattered light [10].

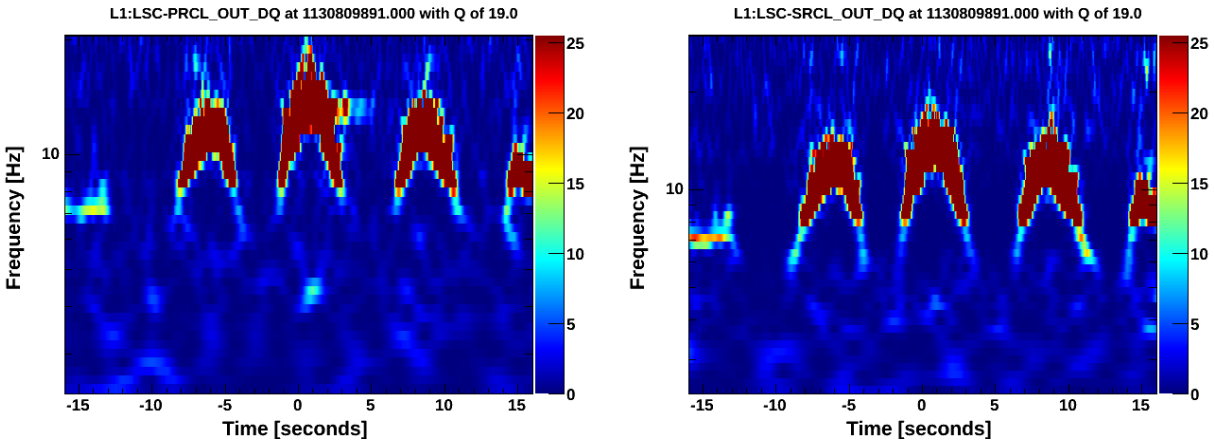

Figure 17: OmegaScan for a glitch seen in both PRCL (right) and SRCL (left).

3.3 Pitch and Yaw Motion

Figure 18 shows 2-dimensional histograms of the signal controlling the motion of one of the signal recycling cavity optics, recorded in pitch and yaw. We observed a large excursion in the control signals at the peak of the elevated ground motion levels.

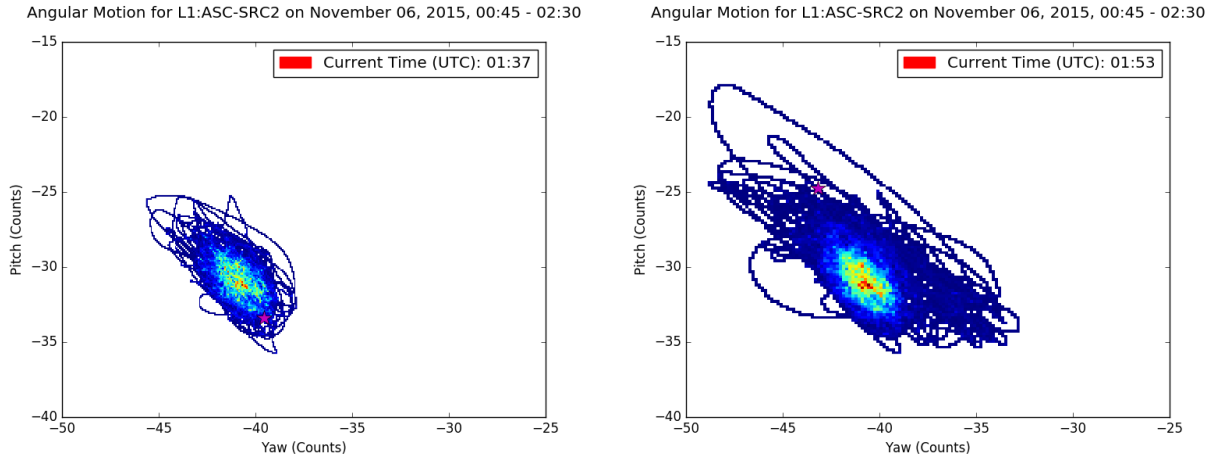

Figure 18: 2-dimensional histograms for the pitch and yaw control signals for SRC2. Excursions from mean represent excess control applied to SR2, which are noticeable particularly during periods of elevated ground motion. The left and right 2D histograms are for the same channel and same lock stretch. The left 2D histogram shows the counts recorded prior to the seismic event shown in the earthquake band BLRMS on the top right in Figure 14. The right 2D histogram was obtained around the time of maximum amplitude for the same seismic event. It was also noticed that the center of the excursions after the seismic event shifted from a mean value centered approximately at the point (-41,-30) to (-41,-31.5). Values on axes are not calibrated.

4 Conclusion

To summarize, we have observed that elevated wind speeds causes elevated noise levels in the ASC control loops at the LIGO Hanford observatory. Optical alignment is critical for the interferometer to maintain its locked state. Furthermore, we have observed that during periods of low wind speeds and low ground motion, we do not observe an overall increase in noise levels or glitches in the ASC control loops.

Elevated ground motion has an effect on the Length Sensing and Control (LSC) channels for the Power Recycling Cavity Length (PRCL) and the Signal Recycling Cavity Length (SRCL) which can be seen as an overall increase in noise levels for frequencies 0.02-0.3 Hz. Glitches with a central frequency of 10 Hz were also observed during elevated ground motion. We also observed in two dimensional histograms, excursions from the mean in the control signals for SRC2 during periods of elevated ground motion. Furthermore, when the elevated ground motion returns to its normal level, we see a shift in the mean in the sensing signals of SRC2.

This study will enable commissioners to further characterize the coupling mechanism which could potentially enable mitigation of the effects of high wind at LIGO-Hanford and high ground motion at both LIGO sites. This could result in improvements in data quality, and the interferometers' sensitivity.

5 Future Work

It would be of interest to see if there have been any broadband acoustic injections that resemble the noise seen during periods of high wind in order to plot spectrograms for ASC control loops. This would help to clarify how acoustic noise couples overall to broadband noise. Furthermore, it would be of interest to look at accelerometers to see if they pick up these vibrations and see where on the interferometer they are the strongest and why. Investigation of potential secondary coupling mechanisms would also be interesting. It is also of interest to examine how and to what extent the buildings housing the interferometers can tilt due to the effects of high winds, and understand how this tilt can couple into ASC control channels.

6 Acknowledgements

I would like to thank Jess McIver, T.J. Massinger and Alan Weinstein for all their help and support. I would also like to thank the Student Faculty Program for organizing this memorable internship, and Josh Smith for his input on my work shown at CSU Fullerton. Finally, I would also like to thank the National Science Foundation.

References

[1] B.P. Abbott et al. (LIGO Scientific Collaboration and Virgo Collaboration). Characterization of transient noise in Advanced LIGO relevant to gravitational wave signal GW150914. *arXiv: 1602.03844* (2016)

[2] B.P. Abbott et al. (LIGO Scientific Collaboration and Virgo Collaboration). Observation of Gravitational Waves from a 22 Solar Mass Binary Black Hole Coalescence. *Phys. Rev. Lett. 116.241103* (2016)

[3] B.P. Abbott et al. (LIGO Scientific Collaboration and Virgo Collaboration). Observation of Gravitational Waves from a Binary Black Hole Merger. *Phys. Rev. Lett. 116. 061102* (2016)

[4] LIGO Scientific Collaboration. Advanced LIGO. *arXiv: 1411.4547* (2014)

[5] B.P. Abbott et al. (LIGO Scientific Collaboration and Virgo Collaboration). GW150914: The Advanced LIGO Detectors in the Era of First Discoveries. *Phys. Rev. Lett. 116. 06131103* (2016)

[6] J. McIver. *The impact of terrestrial noise on the detectability and reconstruction of gravitational wave signals from core-collapse supernovae*. Doctoral dissertation. Retrieved from Scholar Works @ UMass Amherst. Paper 539. (2015)

[7] Github repository holding GWpy python packages. *https://github.com/gwpy/gwpy*

[8] L.K. Nutall et al. Improving the data quality of Advanced LIGO based on early engineering run results. *Class. Quant. Grav. 32, 245005 (2015)*

[9] Link to where OmegaScans were generated. *https://ldvw.ligo.caltech.edu/ldvw/view*

[10] T. Accadia et al. Noise from scattered light in Virgo's second science run data. *Class. Quant. Grav. 27, 19 (2010)*